GEOSCIENCE FRONTIERS 2(2) (2011) 215–221

available at www.sciencedirect.com

China University of Geosciences (Beijing)

GEOSCIENCE FRONTIERS

journal homepage: www.elsevier.com/locate/gsf

ORIGINAL ARTICLE

Mathematical modeling of tornadoes and squall storms

Sergey A. Arsen'yev

Laboratory of Geomechanics, Department of the Earth and Planetary Physics, The Schmidt's Institute of the Earth's Physics, Russian Academy of Sciences (RAS), Bolshaya Gruzinskaya Street, 10, GSP-5, 123995 Moscow D-242, Russia

Received 30 November 2010; accepted 19 February 2011
Available online 5 April 2011

KEYWORDS
Tornadoes;
Squall storm;
Atmosphere boundary layer;
Mathematical modeling

Abstract Recent advances in modeling of tornadoes and twisters consist of significant achievements in mathematical calculation of occurrence and evolution of a violent F5-class tornado on the Fujita scale, and four-dimensional mathematical modeling of a tornado with the fourth coordinate time multiplied by its characteristic velocity. Such a tornado can arise in a thunderstorm supercell filled with turbulent whirlwinds. A theory of the squall storms is proposed. The squall storm is modeled by running perturbation of the temperature inversion on the lower boundary of cloudiness. This perturbation is induced by the action of strong, hurricane winds in the upper and middle troposphere, and looks like a running solitary wave (soliton); which is developed also in a field of pressure and velocity of a wind. If a soliton of a squall storm gets into the thunderstorm supercell then this soliton is captured by supercell. It leads to additional pressure fall of air inside a storm supercell and stimulate amplification of wind velocity here. As a result, a cyclostrophic balance inside a storm supercell generates a tornado. Comparison of the radial distribution of wind velocity inside a tornado calculated by using the new formulas and equations with radar observations of the wind velocity inside Texas Tornado Dummit in 1995 and inside the 3 May 1999 Oklahoma City Tornado shows good correspondence.

1. Introduction

Research on tornadoes is a very wide and "hot" topic in atmospheric and geophysical sciences. Arsen'yev et al. (2010) have recently reviewed works in this field. New results have been obtained by our team at the Institute of the Earth's Physics, the Russian Academy of Sciences (RAS) in Moscow (Arsen'yev et al., 2004a,b; Avetisyan et al., 2008; Gubar' et al., 2008). The most significant achievement is the mathematical calculation of the process of occurrence and evolution of a violent tornado of class F5 on the Fujita scale with velocity of wind from 400 up to 514 km/h. The maximum velocity of a wind reaches 500 km/h at an anomalous pressure of about 250 hPa (mbar) in the center of a tornado (Arsen'yev et al., 2004a,b). A similar event, for

E-mail address: Arsy7@live.ru.

Peer-review under responsibility of China University of Geosciences (Beijing).
doi:10.1016/j.gsf.2011.03.007

Production and hosting by Elsevier

example, the 'Bridge Creek' tornado, took place in Oklahoma, USA, on May 3, 1999 (Monastersky, 1999; Burgess et al., 2002; Dotzek et al., 2003). Even though a storm warning was issued, 48 people lost their lives, 4000 houses were destroyed, a great number of people were seriously injured and the city of Oklahoma suffered significant material losses. Although violent F5-class tornadoes accounted for only 1% of all tornadoes observed in the USA in the 50 years from 1950 to 2000, about 67% of all deaths were caused by this one catastrophic natural phenomenon, and only 5% of strengthened buildings withstand such violent winds without significant damage.

2. Methodology

It should be emphasized that the modeling of violent tornadoes has the following fundamental difficulty: to produce such strong winds it is necessary to consider an energy source, which is equivalent to a nuclear bomb with a power of 20,000 tons of TNT (see detailed calculations in work Arsen'yev et al., 2004b). The methods that are ordinarily used in meteorology (Arsen'yev et al., 2010), can model storm tornadoes of classes F0−F2 with speeds of the wind not exceeding 71 m/s. Such tornadoes originate from the transition of the potential energy of unstable stratification in the kinetic energy of wind. Other energy sources of such tornadoes are shear instability of a gale-force wind in the top (and average) troposphere, and also conversion of the latent heat of condensation in powerful storm clouds. It is possible to show (Arsen'yev et al., 2010) that these energy sources are not enough for the maintenance of catastrophic tornadoes of class F3 and violent tornadoes of classes F4−F5. An additional energy source (Arsen'yev et al., 2004a,b; Gubar' et al., 2008; Arsen'yev et al., 2010) should be that from ensemble of meso-scale multi-eddies with sizes from 0.1 km up to 1 km. They arise on cold fronts in a thunderstorm supercell. Such meso-scale turbulence is generally asymmetric in relation to mirror transformations and it is described by the asymmetric tensor of Reynolds turbulent stresses. Similar turbulence, referred to in physics as helical (or spiral) turbulence (Arsen'yev et al., 2010), possesses the property of a vortical dynamo, i.e., it can concentrate kinetic energy in one big whirlwind, which develops from finer vortical formations at their merging and accretion. In two-dimensional turbulence a process of transfer of energy from fine eddies to big whirlwinds is determined as a red (or return) cascade (Arsen'yev et al., 2010). In this, energy can be transferring in the area of big scales on the whole power spectrum of turbulence. In a helical turbulence the vortical dynamo transfers energy from meso-scale multi-eddies to one big macro - whirlwind with scale $L = E/I$, where $E = (1/2)\ v^2$ is the maximal kinetic energy of turbulence, and I is its helicity (spirality) determined by the formula

$$I = \frac{1}{2V} \iiint_V v\ rot\ v\ \mathrm{d}V,$$

where v is the maximum wind velocity in meso-eddies and V is a concerned volume. The asymmetric turbulence theory with the concept of a vortical dynamo was recently applied by us to calculate a violent class F5 tornado (Arsen'yev et al., 2004a,b, 2010). Next, we constructed a four-dimensional model of a class F1 tornado, which arises from a thunderstorm cloud filled by quickly rotating meso-scale, multi-eddies (Avetisyan et al., 2008; Gubar' et al., 2008; Arsen'yev et al., 2010). The fourth coordinate on the model is the time, multiplied by the characteristic velocity of a wind in tornado. Taking into account the compressibility of air, we calculated a generation by tornado of an infrasound with frequencies from 1 up to 10 Hz (Gubar' et al., 2008). Also, it has been shown that the tornado excites internal gravitational waves possessing its own vorticity.

3. Hypotheses

A possible connection between a tornado and squall storms may be established with the help of an analytical model. A squall storm is characterized by a short-term and strong increase in average velocity of a wind without rotation in areas of heavy storm or at propagation of fast cyclones (Nalivkin, 1969). An example of a squall storm is shown in Fig. 1. We see a strong solitary perturbation (soliton) in the form of a northwest wind with a maximum velocity of 31 m/s against a background of a weak southwest wind. The wind soliton is very narrow. The wind velocity grows from 3 m/s up to 31 m/s for 10 min, and then falls up to 2 m/s within 15 min. A typical time of existence for a squall storm is $t^* = 25$ min. The rotation of air, which is characteristic for tornadoes, is absent (Nalivkin, 1969).

Squall storms have resulted in accidents at sea. In March, 1878, the English frigate "Evridic" was overturned in a squall and sunk instantly together with the crew. The same fate overtook the Russian battleship "Mermaid" on September 19, 1893 in the Baltic Sea, with 178 seamen lost (Nalivkin, 1969). On land, squall storms can destroy poorly constructed and simple buildings and break trees in woods. For example, a squall storm with a velocity up to 35 m/s and duration of only 10 min in a Moscow suburb on May 29, 1937, caused significant destruction of country settlements — trees were overturned together with roots; houses were unroofed, fences demolished; glass in windows was shattered (Nalivkin, 1969). Rotation of an average wind is absent. In San Francisco, on November 21, 1910, a squall storm attacked strengthened city houses. The duration of the storm was only 2 min, with a wind velocity of 100 km/h. Nalivkin (1969) wrote: "As though above city one enormous, long and narrow air wave has flown".

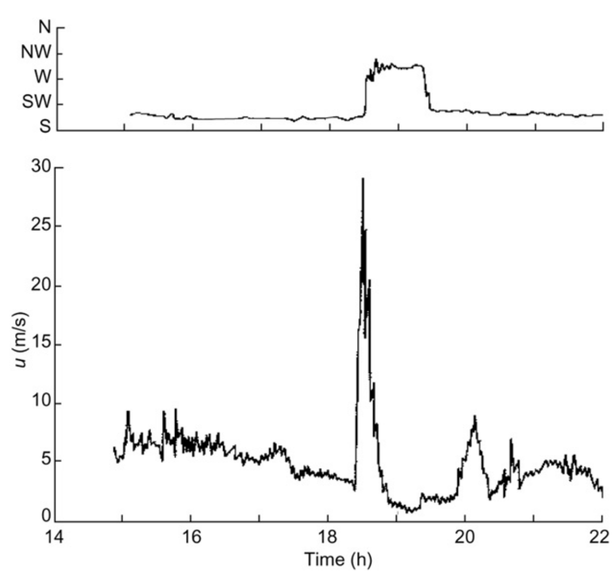

Figure 1 Change of direction (upper) and velocity (lower) of a wind during the passage of a squall storm (after Nalivkin, 1969).

Squall storms are characterized by the presence of clouds that have a thin layer of inversion on the bottom border. Inside the inversion the temperature increases with height, and the outside temperature falls with height (Fig. 2). The inversion appears at the level of condensation, which is near to the bottom border of clouds, because inside the cloud the temperature increases due to the calorification of the latent heat of steam formation. It is essential that the inversion possesses properties of locking. A volume of air, which rises from below in an inversion layer, is colder than ambient air and it is pushed out downwards by Archimedean forces. Similarly, warmer air, which has arrived in an inversion from above, is pushed out upward. Thus, an inversion can be modeled by the surface of the air current $\zeta(x, y)$. Here, horizontal velocities of the wind u and v, can coexist and the vertical velocity w is submitted to the condition

$$\text{If } z=\zeta, \text{ then } w=\frac{\partial\varsigma}{\partial t}+u\frac{\partial\varsigma}{\partial x}+v\frac{\partial\varsigma}{\partial y}. \tag{1}$$

In addition, vertical turbulent stresses on the inversion should be continuous, i.e.:

$$\text{If } z=\zeta, \text{ then } E_x^z=E_x^0, E_y^z=E_y^0, \tag{2}$$

where E_x^z, E_y^z are the turbulent stresses in the nether boundary layer of an atmosphere (NBLA), E_x^0, E_y^0 are the turbulent stresses on the bottom layer of the middle troposphere (MT), ζ is perturbation of a level on an inversion surface, axis z is directed downwards from an unperturbed level $z = 0$, the surface of Earth (SE) is at a level $z = H$ (Fig. 2).

If the inversion in any place is broken by very strong ascending movements, then equation (1) can not take place and air collects into these upwelling plumes, forming powerful thunderstorm clouds (Snow, 1984). If vertical movements are insufficient for destruction of the inversion, then equation (1) takes place, and gravitational waves arise on a surface of the inversion.

The problem of the mathematical description of these waves on an interface between layers with different temperatures and wind velocities in consideration of the compressibility of air was resolved in 1947 by D.L. Laikhtman (see Khrgian, 1984). His solution describes internal waves in the troposphere. However, the basic mode, corresponding to gravitational waves in the atmosphere with a homogeneous density, is omitted in this solution. Nevertheless, this mode appears in the analysis of the Laplace's tidal equations on an atmosphere (Dikiy, 1969). Therefore, the consideration of movements in the NBLA, associated with this wave mode, has practical importance. In given treatise, this problem is solved for long gravitational waves with length of wave λ that considerably exceeds the thickness H ($\lambda \gg H$). In such case we can use the condition of a static atmosphere

$$g\rho=\frac{\partial p}{\partial z}. \tag{3}$$

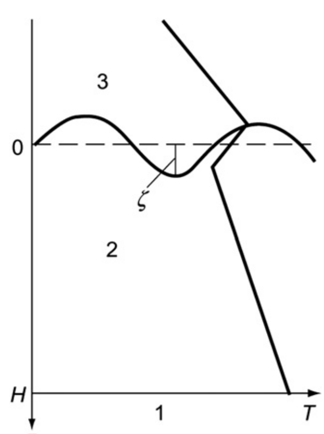

Figure 2 System of coordinates and temperature of air T in the nether boundary layer of atmospheres NBLA (this layer is denoted by number 2), and in the middle troposphere MT (this layer is denoted by number 3). Position of a layer inversion is designated by line ζ; the surface of Earth SE is designated by number 1.

4. The squall storm and its basic equations

The density ρ and pressure of the air p in Equation (3) vary with height. These changes can be calculated from the equation of state

$$p = R_c\rho T, \tag{4}$$

where T is an absolute temperature, $R_c = 287$ m^2/(s^2 °K) is the specific gas constant of dry air. Humidity has no effect on the NBLA at heights below a level of condensation, which practically coincides with the level $z = 0$ (Fig. 2). Since we are interested in movements within the NBLA at $z \geq \zeta$, the influence of humidity for us is inessential. Let us take the logarithm of equation (4) and take the derivative of the result with respect to z. We obtain

$$\frac{1}{p}\frac{dp}{dz}=\frac{1}{\rho}\frac{d\rho}{dz}+\frac{1}{T}\frac{dT}{dz}. \tag{5}$$

Substituting pressure p in equation (5) from equation (4) and a gradient dp/dz from equation (3), we find

$$\frac{g}{TR_c}=\frac{1}{\rho}\frac{d\rho}{dz}+\frac{1}{T}\frac{dT}{dz}.$$

Thus, we obtain a law that defines the change in density with altitude

$$\frac{1}{\rho}\frac{d\rho}{dz}=\frac{1}{T}(\gamma_0-\gamma), \tag{6}$$

where $\gamma = dT/dz$, $\gamma_0 = g/R_c = 3.42 \times 10^{-2}$ °C/m is constant. It is the temperature gradient in atmosphere with a uniform density, because $d\rho/dz = 0$ at $\gamma_0 = \gamma$.

If $\gamma > \gamma_0$, the density of air increases with height, i.e., $d\rho/dz < 0$. This situation is rare. It may occur during intense heating of the NBLA in a summer day. This corresponds to an unstable condition of the atmosphere because heavy (and denser) air is at the top of NBLA, and lighter air is below, i.e., $\gamma > \gamma_0 > \gamma_a$, where $\gamma_a = 10^{-2}$ °C/m is a dry-adiabatic gradient of temperature. Upon cooling of the NBLA in stormy weather $\gamma \cong \gamma_0$, that corresponds to an atmosphere with a homogeneous density. The case $\gamma < \gamma_0$, when the density of air decreases with height, takes place most frequently. For example, it (almost always) is observed above the NBLA, in MT. This corresponds to stable stratification when heavy air is below. Hereinafter, we shall consider case $\gamma \cong \gamma_0$ in which stratification inside of the NBLA is unstable ($\gamma_0 > \gamma_a$). This means that air inside the NBLA becomes turbulent because of convection and vertical shear of the average wind velocity.

A condition $\rho = \text{const}$ allows us to vertically integrate equation (3) from $z = \zeta$ to z and to obtain the law of variation of air pressure with height within the NBLA

$$p = p_0 + g\rho(z - \zeta), \tag{7}$$

where p_0 is pressure at level $z = \zeta$.

Let us direct the x-axis along the wind current at the lower boundary of MT and denote the wind velocity on this border by the letter W. Strong winds in MT lead to a quadratic law of resistance on the inversion. That is,

$$\text{If } z = \zeta, \text{ then } E_x^0 = C_g W^2, \tag{8}$$

where C_g is the coefficient of resistance. In formulas (8) and (2), the tangential wind stress is divided on the air density $\rho = 1.3\ \text{kg/m}^3$. Flows within NBLA, which emerge under the influence of the wind W, are also directed along the x-axis, since we neglect the Coriolis force due to the small thickness of the NBLA: $H \in [500, 2000]$ m. Thus, cross currents along the y-axis become insignificant, and we may write the equations of motion and continuity on the form of

$$\frac{\partial u}{\partial t} = -\frac{1}{\rho}\frac{\partial p}{\partial x} - \frac{\partial E_x^z}{\partial z} + A_L \frac{\partial^2 u}{\partial x^2}, \tag{9}$$

$$\frac{\partial u}{\partial z} + \frac{\partial w}{\partial z} = 0, \tag{10}$$

where A_L is the coefficient of horizontal shear turbulent viscosity. The Equations (9) and (10) contain turbulent stresses and vertical velocities w within the NBLA, which is possible to exclude by vertical integration from $z = \zeta$ to $z = H$. As a result, Equation (10) becomes

$$\frac{\partial \varsigma}{\partial t} = \frac{\partial S}{\partial x}, \tag{11}$$

where $S = \int_\varsigma^H u \, dz$ is full stream. By deriving equation (11), we took into account the boundary conditions as in equations (1) and (2) and the following condition:

$$\text{if} = H, \text{ then } u = w = 0 \tag{12}$$

It is easy to exclude the air pressure from the Equation (9), using the law in equation (7)

$$\frac{1}{\rho}\frac{\partial p}{\partial x} = \frac{1}{\rho}\frac{\partial p^0}{\partial x} - g\frac{\partial \zeta}{\partial x}. \tag{13}$$

It is convenient to present the level of inversion ζ as the sum of the static ζ_s and the dynamic ζ_d components: $\zeta = \zeta_s + \zeta_d$. Then, if the static inclinations of the inversion level are counterbalanced by the pressure gradients upon inversion

$$\frac{1}{\rho}\frac{\partial p_0}{\partial x} = g\frac{\partial \zeta_s}{\partial x},$$

Equation (13) may be written down in the form of

$$\frac{1}{\rho}\frac{\partial p}{\partial x} = -g\frac{\partial \zeta_d}{\partial x}. \tag{14}$$

Substituting equation (14) into equation (9) and omitting the index d (hereinafter we consider only the dynamic inclinations of the level ζ_d), we find

$$\frac{\partial u}{\partial t} = g\frac{\partial \zeta}{\partial x} - \frac{\partial E_x^z}{\partial z} + A_L \frac{\partial^2 u}{\partial x^2}. \tag{15}$$

Let us integrate the Equation (15) by z in limits of NBLA. We obtain

$$\frac{\partial S}{\partial t} = gH\frac{\partial \zeta}{\partial x} - E_x^H + E_x^0 + A_L \frac{\partial^2 S}{\partial x^2}. \tag{16}$$

The system of two Equations (16) and (11) is closed with regards to two unknown values S and ζ, if the turbulent stresses are known on the top and bottom borders of the NBLA or their relationship with S or ζ. This system is the basic equations for mathematical description of squall storms.

5. Modeling of the squall storms

Let's find the solution of system of Equations (11) and (16) in the form of the progressive wave propagating with velocity G, that is $S = F(x + Gt)$. Then the Equation (11) gives the algebraic relationship between S and ζ. Denoting $\chi = x + Gt$, we get (the index χ near F denotes a derivative on χ)

$$\frac{\partial S}{\partial x} = F_\chi; \frac{\partial S}{\partial t} = F_\chi G; \frac{\partial \varsigma}{\partial t} = \frac{\partial S}{\partial x} = F_\chi = \frac{1}{G}\frac{\partial S}{\partial t} = \frac{\partial}{\partial t}\left(\frac{S}{G}\right).$$

From this it follows that (we integrate by time t)

$$S = \zeta G \tag{17}$$

since the constant of integration is equal to zero (when $S = 0$ and $\zeta = 0$). Using the Equation (17), we can exclude level ζ from the Equation (16)

$$\frac{\partial S}{\partial t} = \frac{gH}{G}\frac{\partial S}{\partial x} - E_x^H + E_x^0 + A_L \frac{\partial^2 S}{\partial x^2}. \tag{18}$$

For the frictional stresses on the bottom border of the NBLA it is possible to accept the known law in the theory of long waves (Gill, 1986; Arsen'yev, 1989)

$$E_x^H = f_* S. \tag{19}$$

Here $f*$ is the frequency of the friction, which may be estimated by the formula (Arsen'yev, 1989)

$$f_* = \frac{3A}{H^2(1-n)^2}, \tag{20}$$

where $n = z_0/H$, and z_0 is the height of ledges of a roughness on the surface of the Earth and A is the coefficient of a shear turbulent viscosity. On the other hand, the frictional stresses on the top border of the NBLA are determined by formula (8). In this formula, the velocity of wind W on the bottom boundary of the MT may be connected with the velocity of the wind on the top border of the NBLA u^0 with the help of the ratio

$$u^0 = kW, \tag{21}$$

where k is the wind coefficient. If the velocity of a wind at the transition through inversion does not suffer a break, then $k = 1$. Otherwise we have $0 < k < 1$ since the velocity of a wind decreases with height. Note that the formula (21) is used in the physics of oceans to relate the velocity of a wind in the bottom layer of an atmosphere with the velocity of the current on the ocean surface (Arsen'yev, 1977; Arsen'yev and Felzenbaum, 1977).

The full stream S may be expressed through the wind velocity u^0, if we specify a particular model of the wind velocity distribution with height within the NBLA (logarithmic, parabolic or any other law). The simplest model is the slab-model in which all parts are moving with the same velocity $u^0 = u$, except for a thin near- ground layer of an atmosphere with thickness about 10 m where the wind velocity sharply decreases up to zero. In this case, the friction is concentrated near the level of $z = H$, where the equation (19) takes place. For the slab-model we have $S = uH$ and formula (8) may be written as

$$E_x^0 = \frac{C_g}{k^2 H^2} S^2. \tag{22}$$

Inserting equations (22) and (19) in equation (18), we obtain the Equation for S

$$\frac{\partial S}{\partial t} = \frac{gH}{G}\frac{\partial S}{\partial x} + \alpha S^2 - f_* S + A_L \frac{\partial^2 S}{\partial x^2}, \tag{23}$$

where $\alpha = C_g/k^2H^2$.

Recall now that we are looking for a solution in the form of a progressive wave $S = F_{(\chi)}$. Then $\partial S/\partial t = GF_\chi$, $\partial S/\partial x = F_\chi$, $\partial^2 S/\partial x^2 = F_{\chi\chi}$ and Equation (23) takes the form

$$A_L F_{\chi\chi} + \alpha F^2 - f_* F - G\left(1 - \frac{gH}{G^2}\right) F_\chi = 0. \tag{24}$$

For waves propagating with a velocity of $G = (gH)^{1/2}$, the Equation (24) transforms into equation

$$A_L F_{\chi\chi} + \alpha F^2 - f_* F = 0. \tag{25}$$

This is easy to solve by multiplication by F_χ

$$\frac{A_L}{2}\frac{d}{d\chi}\left[\left(\frac{dF}{d\chi}\right)^2\right] + \frac{\alpha}{3}\frac{dF^3}{d\chi} - \frac{f_*}{2}\frac{dF^2}{d\chi} = 0. \tag{26}$$

Integrating equation (26), we find

$$\left(\sqrt{\frac{3A_L}{2\alpha}}\right) F_\chi = F\sqrt{\beta - F}, \tag{27}$$

where $\beta = (3/2)(f_*/\alpha)$. The constant of integration is equal to zero, because $F \Rightarrow 0$, $F_\chi \Rightarrow 0$ when $\chi \Rightarrow \infty$.

In the Equation (27) variables are dividing

$$\frac{dF}{F\sqrt{\beta - F}} = d\chi\sqrt{\frac{2\alpha}{3A_L}}.$$

Integrating once again, we obtain

$$-\frac{2}{\sqrt{\beta}}\mathrm{Arth}\left(\sqrt{\frac{\beta - F}{\beta}}\right) = \chi\sqrt{\frac{2\alpha}{3A_L}}.$$

or

$$\sqrt{\frac{\beta - F}{\beta}} = -\,\mathrm{th}\left(\chi\sqrt{\frac{\alpha\beta}{6A_L}}\right). \tag{28}$$

Substituting identity $\mathrm{th}^2 x \equiv 1 - \mathrm{sech}^2 x$ in equation (28), we obtain

$$\frac{\beta - F}{\beta} = 1 - \mathrm{sech}^2\left(\chi\sqrt{\frac{\beta\alpha}{6A_L}}\right).$$

Thus,

$$S = F = \beta\,\mathrm{sech}^2(\chi/\Delta), \tag{29}$$

$$u = (\beta/H)\,\mathrm{sech}^2(\chi/\Delta), \tag{30}$$

$$\zeta = \left[\beta/(gH)^{1/2}\right]\mathrm{sech}^2(\chi/\Delta), \tag{31}$$

where

$$\Delta = \sqrt{\frac{4A_L}{f_*}} = H(1-n)\sqrt{\frac{4A_L}{3A}} \tag{32}$$

is the width of the solitons (29)–(32).

Using the solutions (31) and (7), we find the changes of pressure in the NBLA

$$p = p_0 + g\rho z - g\rho\frac{\beta}{\sqrt{gH}}\mathrm{sech}^2\left(\frac{\chi}{\Delta}\right). \tag{33}$$

In particular, on the Earth's surface, when $z = H$

$$P = p_0 + g\rho H - g\rho\frac{\beta}{\sqrt{gH}}\mathrm{sech}^2\left(\frac{\chi}{\Delta}\right). \tag{34}$$

Equations (34) and (30) show that during the passage of a squall storm the pressure falls, and the wind velocity grows. The time duration of a squall storm may be estimated by the formula

$$t_* = \frac{\Delta}{G} = \sqrt{\frac{4A_L}{gf_*H}}. \tag{35}$$

As an example. Fig. 3 shows calculations of the oscillations of the near-ground wind velocity from the following values of parameters: $C_g = 10^{-2}$, $k = 0.7$, $H = 980$ m, $p_0 = 888.4$ hPa, $g = 9.8$ m/s^2, $\rho = 1.3$ kg/m^3, $z_0 = 0.05$ m (grass, rye), $A = 129.7$ m^2/s, $A_L = 2.16 \times 1000000$ m^2/s. In this case $\Delta = 147 \times 1000$ m, $\beta = 30380$ m^2/s, $\alpha = 2.08 \times 10^{-8}$. From Fig. 3, we see that the maximum wind velocity reaches 31 m/s and the time of its passage in accordance with equation (35) is 25 min, which corresponds to observations (Fig. 1). The width of the soliton is equal to 147 km. Thus, a squall storm is a meso-scale atmospheric phenomenon that occurs during hurricane winds in the middle troposphere. In our example the maximum value of W is 44.3 m/s.

6. Tornado caused by squall storm

It is essential that the squall storm soliton, propagating along subcloud inversions, can get into a storm meso-cyclone having

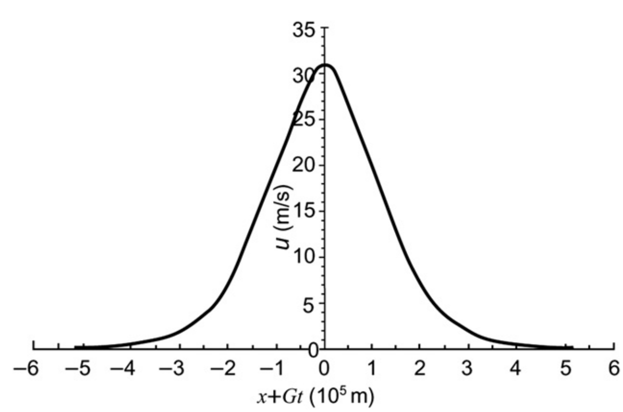

Figure 3 Variation of velocity of a wind u at a surface of the Earth in the passage of a squall storm. The maximum velocity is equal to 31 m/s.

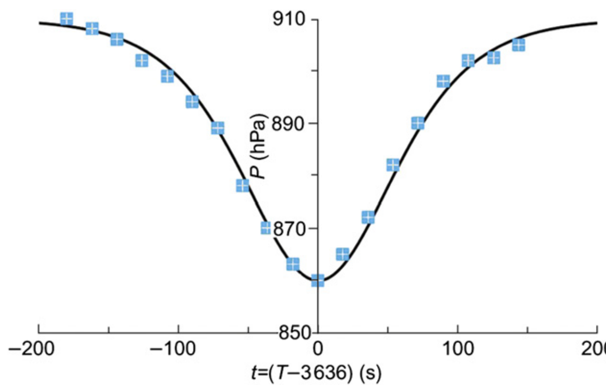

Figure 4 Variation of pressure P at a surface of the Earth during the passage of a tornado, 8 Jun 1995 near Allison, TX (Winn et al., 1999). The measured, averaged pressures are shown by small squares. The thick theoretical curve calculated by the help of formula (37).

weak rotation, caused by shear instability (Arsen'yev et al., 2000; Arsen'yev et al., 2010). In this case the soliton is captured by a meso-cyclone because strong ascending movements on the thunderstorm front destroy temperature inversion within the meso-cyclone. Rotation of the air inside the meso-cyclone is described by cyclostrophic balance (Arsen'yev et al., 2010)

$$\frac{\partial p}{\partial r}=\rho\frac{v^2}{r}, \tag{36}$$

where r is the radial coordinate directed from the center of rotation to outside. Thus, the squall storm can cause an additional pressure drop within the thunderstorm supercell and it can amplify the wind rotation, as a result generating a tornado.

Obviously, to estimate air pressure and velocities of a wind within an arising tornado it is necessary to substitute the formula (34) at $x = r$ in the equation (36) and to resolve this equation concerning azimuth velocity v. Finally we shall obtain

$$P=p_0+g\rho H-g\rho\frac{\beta}{\sqrt{gH}}\mathrm{sec\,h}^2\left(\frac{r+Gt}{\Delta}\right), \tag{37}$$

$$v=\mathrm{sec\,h}\left(\frac{x+Gt}{\Delta}\right)\sqrt{\frac{2g\beta r}{G\Delta}\mathrm{th}\left(\frac{x+Gt}{\Delta}\right)}. \tag{38}$$

Formulas (37) and (38) give solution of the problem about mathematical description of the wind velocity and the air pressure in developing tornado.

For a check of the solution (37) we have involved results of measurements of air pressure in a June 8 1995 tornado near Allison, TX, in the eastern Texas panhandle (Winn et al., 1999). The average values of the measured pressure are shown on Fig. 4 by small squares. On that figure we have shown the thick theoretical curve calculated by the help of formula (37). For calculations we have chosen the following values of parameters: $C_g = 0.02, k = 1, H = 980$ m, $p_0 = 785.15$ hPa, $g = 9.8$ m/s^2, $\rho = 1.3$ kg/m^3, $z_0 = 0.05$ m (grass, rye), $A = 1.709$ m^2/s, $A_L = 67.32$ m^2/s. In this case $\Delta = 7101.82$ m, $\beta = 384.62$ m^2/s. For convenience we have entered a theoretical time $t = T$(s) − 3636 s (here T is the current time of measurements shown by the device). The calculated results coincide well with the observed ones.

On Fig. 5 a thick black line shows variation of the velocity of a wind within the upcoming tornado calculated with using Equation (38). For calculations we have chosen the following values of parameters: $C_g = 0.02, k = 1, H = 980$ m, $g = 9.8$ m/s^2, $\rho = 1.3$ kg/m^3, $z_0 = 0.05$ m (grass, rye), $A = 300$ m^2/s, $A_L = 3.96$ m^2/s. In this case $\Delta = 130$ m, $\beta = 67500$ m^2/s. Small red squares are measurements of the wind velocities within a tornado of class F2 using meteorological radars in the USA (Wurman and Gill, 2000). Fig. 5 shows that capture of a soliton of a squall storm by a thunderstorm supercell has led to formation of a catastrophic tornado of class F2 with the maximal wind velocity 65 m/s. On Fig. 5, we see that on the observed curve there are additional maximums of the wind velocity (at $r \approx 300$ m, $r \approx 650$ m, $r \approx 780$ m, $r \approx -500$ m, $r \approx -780$ m). It is obvious that these maximums are related to large-scale meso-scale turbulent eddies which fill up the tornado. Thus, in this case, the tornado is multi - vortical and attenuation of the wind velocity occurs more slowly than in theoretical cases.

Arsen'yev et al. (2010) proved that meso-scale eddies within a tornado in the course of time miniaturize their own dimensions, kinetic energy and angular moment. Therefore, we have considered one more example of calculations as applied to the violent tornado

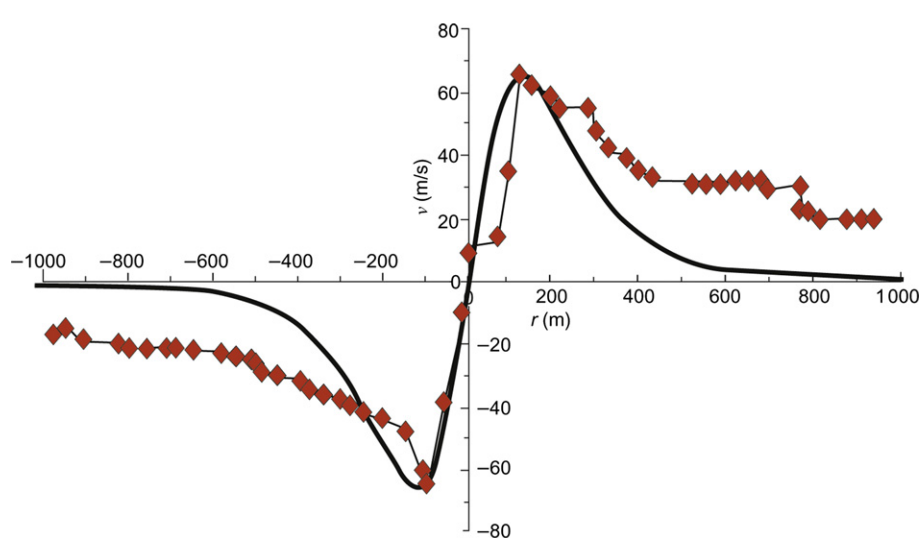

Figure 5 Comparison of a theoretical radial distribution of the average azimuthal wind velocity inside an F2 tornado calculated using Equation (37) (a black line) with radar measurements of the wind velocity inside a tornado (small squares).

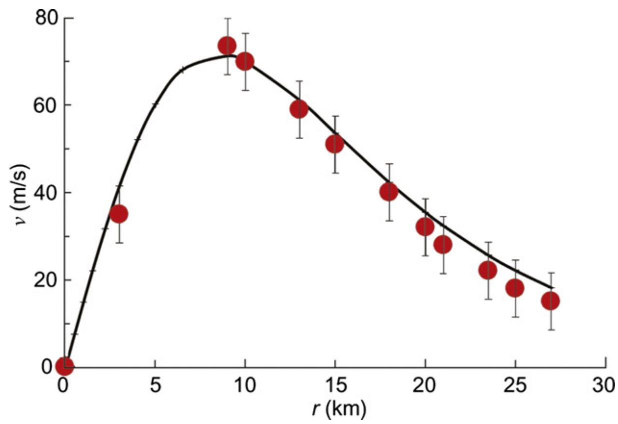

Figure 6 Comparison of a theoretical radial distribution of the average azimuthal wind velocity within an F5 tornado calculated using Equation (38) (a black line) with radar measurements of the wind velocity within a tornado (small circle). Vertical lines point the 10% exactness.

F5. Small circles on Fig. 6 show results of observations of a tornado in Oklahoma on May 3 1999 using meteorological radars (Wurman et al., 1996, 1997; Monastersky, 1999; Burgess et al., 2002). The thick black line shows results of calculations with the help of formula (38). Values of parameters are: $C_g = 0.02$, $k = 1$, $H = 980$ m, $g = 9.8$ m/s^2, $\rho = 1.3$ kg/m^3, $z_0 = 0.05$ m (grass, rye), $A = 355.55$ m^2/s, $A_L = 19591.84$ m^2/s. In this case $D = 8400$ m, $\beta = 80000$ m^2/s. Evidently, the theory and observations are coincident within the limits of 10% exactness.

7. Conclusions

Let us formulate the main results obtained in this work.

1. A theory of squall storm is constructed. A storm is modeled by a running perturbation of the temperature inversion on the lower boundary of cloudiness. This perturbation is induced by the action of hurricane winds in the upper and middle troposphere, and looks like a progressive solitary wave (soliton).
2. A theory of stimulation of tornado by squall storms is created. If a soliton of a squall storm gets into a thunderstorm supercell then the soliton is captured by the supercell resulting in amplification of the wind velocity and an additional pressure fall of air inside the storm supercell. Finally, a cyclostrophic balance generates a tornado. A comparison of the radial distribution of the wind velocity inside a tornado, which was calculated with the help of the equations of given treatise, with the real radar observations of wind velocity inside the Dummit Texas tornado, 2 June, 1995 shows a very good correspondence.
3. Verification of the theory was realized for observations of air pressure in a tornado on 8 June, 1995, near Allison, Texas and for radar data for wind velocity of the 3 May 1999 Oklahoma City Tornado. The theory corresponds to observations within 10% precision.

Acknowledgments

I thank Academicians G.S. Golitzin and Victor I. Starostin for their interest in my work and for useful discussion. The authors are grateful to Prof. Hualin Zeng for his help on language editorial efforts. This work was supported by the Presidium of the Russian Academy of Sciences in the framework of the theme 'Disasters'.

References

Arsen'yev, S.A., 1977. Numerical modelling of the upper active ocean layer. Izvestiya Akademii Nauk SSSR, Atmospheric and Oceanic Physics 13 (12), 1325–1330 (in Russian with English abstract).
Arsen'yev, S.A., 1989. Dynamics of Shelf Water. State Publishing House "Mosc.Gos.Universitet", Moscow, p. 96 (in Russian).
Arsen'yev, S.A., Babkin, V.A., Gubar', A.Y., Nikolaevskiy, V.N., 2010. The Theory of Meso-Scale Turbulence. Eddies of Atmosphere and Ocean. Publishing House "Regular and Chaotic Dynamics", Moscow - Izhevsk, p. 362 (in Russian with English abstract).
Arsen'yev, S.A., Felzenbaum, A.I., 1977. Integral model of the upper active ocean layer. Izvestiya Akademii Nauk SSSR, Atmospheric and Oceanic Physics 13 (10), 1034–1042 (in Russian with English abstract).
Arsen'yev, S.A., Gubar', A.Y., Nikolaevskiy, V.N., 2004a. Self-organizing of the tornadoes and hurricanes in atmospheric currents with meso-scale eddies. Doklady Akademii Nauk 396 (4), 541–546 (in Russian with English abstract).
Arsen'yev, S.A., Gubar', A.Y., Nikolaevskiy, V.N., 2004b. Beginning and evolution of a tornadoes and hurricanes as the phenomena of self-organizing of meso-scale whirlwinds. In: Gliko, O.A. (Ed.), Researches in the Field of Geophysics. To the 75-anniversary of the United O.U. Schmidt's Institute of Physics of the Earth. UIPE of the Russian Academy of Sciences, Moscow, pp. 365–371 (in Russian with English abstract).
Arsen'yev, S.A., Nikolaevskiy, V.N., Shelkovnikov, N.K., 2000. Eddy non-stability and beginnings of the tornadoes and spouts. Vestnik Moskovskogo Universiteta. Ser. 3: fizika i astronomiya 1, 50–53 (in Russian with English abstract).
Gubar', A.Yu., Avetisyan, A.I., Babkova, V.V., 2008. Tornado rise 3D numerical model in the mesoscale turbulence theory of Nikolaevskiy. Doklady Akademii Nauk 419 (4), 547–552 (in Russian with English abstract).
Avetisyan, A.I., Babkova, V.V., Gaysaryan, S.S., Gubar', A.Y., 2008. Development of the parallel software for the decision of a three-dimensional problem about a birth of a tornado using the Nikolaevskiy's theory. Mathematical Modelling 20 (8), 28–40 (in Russian with English abstract).
Burgess, D.W., Magsig, M.A., Wurman, J., Dowell, D.C., Richardson, Y., 2002. Radar observations of the 3 May 1999 Oklahoma City Tornado. Weather and Forecasting 17, 456–471.
Dikiy, L.A., 1969. The Theory of Fluctuations of a Terrestrial Atmosphere. Hidrometeoizdat, Leningrad, p.196 (in Russian with English abstract).
Dotzek, N., Griesler, J., Brooks, H.E., 2003. Statistical modelling of tornado intensity distributions. Atmospheric Research 67–68, 163–187.
Gill, A., 1986. Atmosphere – Ocean Dynamics. Mir, Moscow, 2 volumes, p. 816 (in Russian).
Khrgian, A.Kh., 1984. Physics of the Atmosphere. Hidrometeoizdat, Leningrad. 2 volumes, p.568 (in Russian with English abstract).
Monastersky, R., 1999. Oklahoma tornado sets wind record. Science News 155 (2), 308–309.
Nalivkin, D.V., 1969. Hurricanes, Storms and Tornadoes. Publishing House "Nauka", Leningrad, p.488 (in Russian).
Snow, D.T., 1984. Tornado. Scientific American 44 (6), 86–97.
Winn, W.P., Hunyady, S.J., Aulich, G.D., 1999. Pressure at the ground in a large tornado. Journal of Geophysical Research 104 (D18), 22067–22082.
Wurman, J., Gill, S., 2000. Finescale radar observations of the Dummit, Texas (2 June 1995) tornado. Monthly Weather Review 128 (7), 2135–2164.
Wurman, J., Straka, J.M., Rasmussen, E.N., 1996. Fine – scale Doppler radar observations of tornadoes. Science 272, 1774–1777.
Wurman, J., Straka, J.M., Randall, M., Zahray, A., 1997. Design and deployment of a portable, pencil-beam, pulsed 3-cm Doppler radar. Journal of Atmospheric and Oceanic Technology 14, 1502–1512.